IEEE Access
Multidisciplinary | Rapid Review | Open Access Journal

Received May 15, 2019, accepted May 23, 2019, date of publication May 28, 2019, date of current version June 17, 2019.

Digital Object Identifier 10.1109/ACCESS.2019.2919507

An Improved Differential Evolution Algorithm for Optimal Location of Battery Swapping Stations Considering Multi-Type Electric Vehicle Scale Evolution

SHOUXIANG WANG[1], (Senior Member, IEEE), LU YU[1], (Student Member, IEEE), LEI WU[2], (Senior Member, IEEE), YICHAO DONG[1], AND HONGKUN WANG[1]

[1]Key Laboratory of Ministry of Education, Tianjin University, Tianjin 300072, China
[2]Stevens Institute of Technology, Hoboken, NJ 07030, USA

Corresponding author: Shouxiang Wang (sxwang@tju.edu.cn)

This work was supported in part by the Project of Science and Technology Project of SGCC under Grant 5204JY180003.

ABSTRACT Scientific scale forecasting of multi-type electric vehicles (EVs) is critical to accurately analyze the planning and operation of battery-swapping stations (BSSs) and charging stations (CSs). This paper predicts the proportions of plug-in electric vehicles (PEVs), hybrid electric vehicles (HEVs), and battery-swapping electric vehicles (BSEVs) in the total EV fleet in multi-scenarios via a system dynamics (SD) method. Relying on the predicted evolution scale of the BSEVs and the service demand of BSSs calculated by the service radius (SR) method, an improved differential evolutional algorithm combing with Monte Carlo searching (IDEA-MCS) method is proposed to obtain the optimal location of BSSs in a certain region in Beijing, which achieves an economic optimum of BSSs under the battery-swapping mode (BSM) via centralized charging and unified distribution (CCAUD). The analytical results show that the proportion of the BSEVs in different scenarios is the major driver that impacts the location of BSSs. The distribution of BSSs' BS demand in the optimistic scenario is more inhomogeneous than that in the other scenarios. In addition, a cross-comparison of optimal profits in different scenarios is conducted to verify the optimality of BSS locations for a given scenario. Finally, the proposed IDEA-MCS method is compared with the DEA method and IDEA method to verify its optimality.

INDEX TERMS Battery-swapping station (BSS), differential evolution algorithm, optimal location, system dynamics (SD) method.

NOMENCLATURE

PF_{Class}	Preference factors of EV
$EV_{\text{Class}}(t)$	EV scale at time t
$EVS_{\text{Class}}(t)$	EV scrap amount at time t
$EVP_{\text{Class}}(t)$	EV purchase amount at time t
$UY_{\text{Class}}(t)$	utilization years of EV at time t
$EVA(t)$	Total purchase amount of EV at time t
$EP_{\text{C}}(t)$	Basic electricity price at time t
$EP_{\text{R}}(t)$	Retail electricity price at time t
C_{PM}	Charging/BS profit margin
$PSE(t)$	Basic service cost at time t
CC_{Class}	Actual electricity price
IOC_{Class}	Coefficient of investment and operation cost
MI_{Class}	Coefficient of electricity consumption
$PSI(t)$	Coefficient of policy subsidies at time t
$CFA_{\text{Class}}(t)$	Number of charging/BS facilities at time t
PA_{Class}	Planned number of charging/BS facilities
$EVPR_{\text{Class}}$	Expected vehicle pile or vehicle station ratio
$AVPR_{\text{Class}}$	Actual vehicle pile or vehicle station ratio
EXA_{Class}	Additional part of facilities
$EM_{\text{Class}}(t)$	Endurance mileage at time t
$CA_{\text{Class}}(t)$	Charging/BS accessibility at time t
$CT_{\text{Class}}(t)$	Charging/BS time at time t
$UL_{\text{Class}}(t)$	Utilization life at time t
$RBE_{\text{Class}}(t)$	After-sale service at time t
$PP_{\text{Class}}(t)$	Purchase price at time t

The associate editor coordinating the review of this manuscript and approving it for publication was Ahmad Elkhateb.

$PPS_{\text{Class}}(t)$	Policy subsidies for purchasing EVs at time t
$DP_{\text{Class}}(t)$	driving price at time t
$TD_{\text{EM}}(t)TD_{\text{CT}}(t)$, $TD_{\text{UL}}(t)$, $TD_{\text{PP}}(t)$	Coefficients of technology development for endurance mileage, charging/BS time, utilization life, and purchasing price at time t
$GP_{\text{R}}(t)$	Retail gasoline price at time t
$f^i_{class}(t)$	Preference weight of factor i at time t
$\beta_i(t)$	Conversion coefficient of factor i at time t
θ_{EP}, θ_{GP}	Conversion weights of $EP_{\text{R}}(t)$ and $GP_{\text{R}}(t)$
R_{BSS}	Service radius of BSS
P_{BS}	BS possibility
$R_{\max}$	Maximum service radius
$F^j_{SC,i}$	Service accessibility factor for the ith BSS in location j
F^j_{SC}	Service accessibility factor for the ith BSS in the entire region
L	Total number of optimal planning locations of BSS
N	Total number of planned BSSs
D_{BSS}	Distance from a certain location to one BSS
I_{BSS}	The number of all accessible BSSs
$P_{\text{R,BSS}}$	Regional service coverage range of BSSs
C^j_R	Judgement parameter of accessible BSSs at location j
$C_{\text{R,i}}$	Service degree of the ith BSS
$\text{C}_{\text{R,Total}}$	Total number of selectable locations in the entire region
$P^j_{L,BS}$	The spatial distribution possibility of BSEV in location j
$P^i_{L,Vel}$	The traffic flow of vehicles in location i
T^j_{BS}	Distribution number of BSEVs in location j
S_{EV}	Extension coefficient of EVs
I_{Re}	Regional index
I_{Co}	Competitive index
N_{BS}	Predicted BSEV scale
$F_{\text{Loc,i}}$	Scope of service ratio in the ith BSS
$S_{\text{BSS,i}}$	BS demands in the ith BSS
$C_{\text{R,max}}$	The maximum range of BSS
$C_{\text{L,out}}$	Overrange coefficient
T_{hour}	BS time
L_{BSS}	Number of BS lanes in BSS
Q_{max}	The maximum BS number in an hour in each BSS
S_{Land}	Coverage size of BSS
$C_{\text{Land,j}}$	Land price per square meter at location j
I_{Land}	Investment land cost of BSS
I_{Eq}	Investment of BSS equipment cost
I_{In}	Investment of land occupation cost
C	Battery capacity
H_{B}	Battery cost per BS
C_{B}	Battery price of BSEV
C_{BS}	Service price per BS
C_{Re}	Battery rental cost per month
W_{Mon}	Average number of weeks in each month
$C_{\text{Pro,per}}$	BS profits for BSSs per week
$C_{\text{Op,per}}$	BS cost for BSSs per week
I_{C}	Annual operating converted profit
I_{Total}	Total annual converted investment
r_0	Discount rate
y_{c}	The year of depreciation
M_{Week}	Weekly mileage
D_{E}	Mileage per kilowatt hour
D_{Sea}	Seasonal coefficient
P_{An}	Annual converted net profit
$v_{i,j}(t)$	The jth individual in the ith population of mutation operators in the tth iteration
$p_{i,j}(t)$	The jth individual in the ith population of father generation in the tth iteration
$g(t)$	Dynamic factor in the tth iteration
GEN	Number of iterations
$u^s_{i,\text{Sn}}(t)$	The jth individual created by MCS in the tth iteration
F_{S}, F^i_P	Penalty coefficient of I_{C}
$R_{\text{I}}(t)$	Growth rate at time t

I. INTRODUCTION

As one of the representative renewable vehicles, electric vehicle (EV) has attracted significant attentions for the potential environmental benefits. Meanwhile, the EV industry has become an important part on promoting the development of renewable energy industry and accelerating the transformation of energy structure [1].

Currently, two categories of EVs are available on the market, which are hybrid EV (HEV) and all-EV (AEV) [3]. For AEVs, plug-in EV (PEV) and battery-swapping EV (BSEV) are two main types of AEVs. In the transitional process on realizing the transformation of energy structure, driving HEVs powered by both gas and electricity would be cheaper and more environmentally friendly, compared with traditional internal combustion engine vehicles [4]. Meanwhile, for the demand of electric energy supply, direct charging mode (DCM) is a popular mode for PEVs and HEVs, because the charging facilities are more accessible. However, the disordered charging of EVs by DCM will make adverse impacts on the power grid operation, including fluctuations of load, voltage, and frequency [6]. To this end, the battery-swapping mode (BSM) shows obvious advantages as an alternative way

compared with DCM [7]. On the one hand, the EV users need not to purchase batteries directly so the initial purchase price of BSEV is lower for them. Moreover, a systematic battery management achieved in BSM contributes to the effective maintenance of batteries and the extension of the battery lifetime. On the other hand, EV users spend only several minutes to swap batteries in a battery-swapping station (BSS), while typically it will take several hours for slow direct charging (DC) or at least tens of minutes for fast DC in DCM [8]. Besides, several regions and companies in China have been spreading BSM [9]–[11]. For example, 27 BSSs were taken into operation by 2014 in Hangzhou, which have served 723 EVs [9]. 253 electric taxis had been served by BSSs in Haikou by 2014 [10]. Additionally, the State Grid Corporation of China proposed a development strategy for BSSs in 2012, and 191 BSSs had been constructed by the end of 2015 [11]. Specially, a BSM via centralized charging and unified distribution (CCAUD) for batteries was proposed in 2011 [16]. A centralized charging station (CCS) is built for charging batteries and then distributes the full-charged batteries to each BSS, which could further release the power system's pressure caused by the decentralized charging of EVs. Therefore, BSM is becoming an important way to replenish energy for EVs [12].

From 2000 to 2017, the car ownership has increased to a historical high level in China. Especially, the scale of vehicles in Beijing is sharing a rapid rising speed during this period, which increased from about 1 million in 2000 to more than 6 billion in 2017 [13]. However, currently the EV scale is still small. Both BSM and DCM indicate a low profitability even promoted by the government incentives. Therefore, all categories of EVs need to be improved by developing profitable business models and expending local EV market scale [14]. While analyzing the problems of EVs, many studies assume that the EV scale is fixed [15]–[17]or the upper and lower bounds on the number of EVs are given [18]. Obviously, these assumptions on the EV scale are rough. As BSM is in the early stage of development, the BSSs for taxis and buses are relatively easy to extend, considering the utilization ratio of BSEV and investment cost of BSS. Some researches of BSSs focus on taxis [19], [20], buses [21]–[23], and a combination of two [24]. However, the scale of taxis and buses only takes a small portion of the whole vehicle population. The analysis of BSS based on the scale of EVs, including private EVs is rather limited. Because the simplified models linearize or over-simplify the evolution process of EV scale, such studies are not accurate enough. To this end, a reliable and accurate prediction of EV scale needs to be conducted first. In view of the issue of EV scale prediction, relevant researches have been carried out [25]–[33]. Among them, system dynamics (SD) method [25], [26], multi-agent method [27], [28], analytic hierarchy process (AHP) and logit method [29], [30] are used to predict the EV scale, and the evolutional algorithm (EA) dynamics including SD method is proved to bring great values in application [31]. Meanwhile, policies, consumers' willingness, batteries, and some other relative influences are taken into consideration according to corresponding proportion weights. As an example, multi-layer correlation information is extracted from a limited number of questionnaires through matching the probabilistic distributions of their willingness [32]. Most analyses on predicting EV scale regard all EVs as a single type. Thus, the predicted results cannot reflect specific scales of BSEV, PEV, and/or HEV. Before dealing with the problems of BSSs, an accurate predicted BSEV scale will help conduct more precise and optimal studies of BSS related problems, which will be valuable for investors and governments as well.

After that, with a given reasonable BSEV scale, the geographical distribution problem is mostly considered to deal with the BS demand of BSSs [33], [36]. Some researches focus on the location-routing problems between BSSs and BSEVs to satisfy BS demand as much as possible via optimization algorithms [33]–[35]. Besides, the customers' behavior and psychology are considered to evaluate customers' satisfaction with purchasing EVs [36]. Considering the high investment and a small BSEV scale at present, the accurate data of geographical distribution of traffic flow will contribute to estimate the BS demand of BSSs and optimize the location of BSSs.

Some studies have been carried out on the optimal problems of BSSs or CCSs. An equilibrium framework is proposed to optimally deploy the public charging stations for PEVs while considering public charging opportunities, electricity price, destination and so on [37]. To optimize locations of CCSs among BSSs in the network, a multi-objective programming model is proposed, in which three non-homogenous objectives are considered and calculated by the NSGA-II algorithm [38]. In addition, optimal strategies have been proposed based on different types of objectives and constraints to mitigate high energy losses, enhance the stability and reliability of operation, or improve the economy of investment and operation in distribution system or microgrid (MG) [39]–[45]. However, only a few studies consider the collaborative location of multiple BSSs. According to the above studies, considering the lack of scale evolution of multi-type EV and location of multiple BSSs, this paper proposes an optimal approach for the location of multiple BSSs in a certain region, which combines with a prediction of multi-type EV scale and a calculation method of BS demands under the BSM via CCAUD. The main contributions of this paper are as follows. 1) The scales of multi-type EVs are predicted in multi-scenarios via SD method, which derives precise prediction of BSEV scale that can be used for the optimal location of BSSs in a region. 2) A service radius (SR) method is proposed for estimating the regional service demands of BSSs while considering the regional vehicle proportion and traffic flows, as well as temporal and spatial distributions of vehicles based on the BSEV scale in different scenarios. 3) An improved differential evolutional algorithm combing with Monte Carlo searching (IDEA-MCS) method is presented for the multi-objective optimal collaborative location of BSSs in a real region. Considering the operating profits of

BSSs and the initial investment cost, the locations and profits of BSSs in different scenarios are analyzed. The IDEA-MCS method is finally compared with IDEA method and DEA method to illustrate its improved optimization performance.

The rest of this paper is organized as follows. Section III introduces the SD method for predicting multi-type EV scales. Section IV proposes a SR method for estimating BS demand of BSSs while considering the spatial-temporal distribution of traffic flows. Section V presents an IDEA-MCS method for the regional optimal location of BSSs. Section VI calculates the scales of three types of EVs in three evolutional scenarios as well as optimal location and profit results of BSSs in different evolutional scenarios based on the data of Beijing City in China. The results of IDEA-MCS method are compared with DEA method and IDEA method. Finally, the discussion, conclusion, and prospect are described in Section VII.

II. MULTI-TYPE EV SCALE EVOLUTION ANALYSIS BY SYSTEM DYNAMICS METHOD

SD method combines control theory with feedback theory to study the structure and behavior of system feedback, which was proposed by Forrester in the 1960s. Its main idea is to form a whole system based on a given goal by the organic combination of multiple interdependent factors. The system includes multiple independent factors, which are linked to certain extent to constitute a feedback system. Any complex system can be decomposed into several subsystems, while each subsystem contains state variables, rate variables, and auxiliary variables. The interaction between external factors and internal factors constitutes the driving force of system development, which can be quantified by causality. The main characters of the SD method are the combination of qualitative analysis and quantitative analysis, the rational abstraction of the problem on the basis of statistical data, and the construction of relevant equations to obtain accurate data results [46].

A. SELECTION OF MULTI-TYPE EV SCALES BY SD METHOD

The scale evolution of EVs is complex, which is affected by various factors such as economy, technology, policy, infrastructure for charging/BS, environmental protection pressure, and so on. Based on the data of the EV purchase intention survey [25], the factors such as endurance mileage, driving price, purchasing price, and charging/BS time are selected. Meanwhile, after-sale service, charging/BS accessibility, as well as utilization years of EVs are considered as higher priorities of consumers. After-sale service mainly refers to the cost of replacing the battery after purchasing an EV. These 7 factors are chosen as the preference factors of EVs. Because importance degrees of these individual factors are different, the weights of different factors are as shown in Table 1 suggested by [47]. Besides, the ratios of five preference factors are acquired from existing survey [25] and the other two are shown in Table 2, in which the weight ratios of utilization life and after-sale service are based on the statistical results of 216 questionnaires.

TABLE 1. Weights of EV preference factors.

Preference factors	Weights
Endurance mileage	0.1852
Charging/BS accessibility	0.1806
Charging/BS time	0.1759
Utilization life	0.1296
After-sale service	0.1157
Purchase price	0.1111
Driving price	0.1019

TABLE 2. Weight ratios of two factor items.

Factor item	Psychological options	Weight ratios (%)
Utilization life (year)	0-7	29.1
	7-10	34.5
	>10	36.4
After-sale service (10^4 yuan)	0-1	89.3
	1-3	8.9
	>3	1.8

As three types of EVs are considered, the model is separated into three parts including PEV, HEV, and BSEV, which are connected by the preference factors of EVs. Each part is composed of three submodules, including EV demand module, electricity price, charging/BS facility module, and EV preference factor module. Figure 1 shows the SD model of EVs. The coupling relationship among three parts of preference factors is shown in (1). PF_{PI}, PF_{H}, and PF_{BS} respectively represent the preference factors of PEV, HEV, and BSEV.

$$PF_{\mathrm{PI}} + PF_{\mathrm{H}} + PF_{\mathrm{BS}} = 1 \tag{1}$$

B. EV DEMAND MODULE

Each kind of EV scale $EV_{\mathrm{Class}}(t)$ is decided by the scrap amount $EVS_{\mathrm{Class}}(t)$ and purchase amount $EVP_{\mathrm{Class}}(t)$. $EVS_{\mathrm{Class}}(t)$ is influenced by utilization years $UY_{\mathrm{Class}}(t)$ and $EV_{\mathrm{Class}}(t)$. $EVP_{\mathrm{Class}}(t)$ is decided by $EVA(t)$ and preference factor of EVs $PF_{\mathrm{Class}}(t)$. Subscripts P, H, and BS are respectively used to represent variables for PEV, HEV, and BSEV. The relative equations are shown as in (2)-(4).

$$EV_{\mathrm{Class}}(t) = EV_{\mathrm{Class}}(t-1) + EVP_{\mathrm{Class}}(t) - EVS_{\mathrm{Class}}(t) \tag{2}$$

$$EVS_{\mathrm{Class}}(t) = \frac{EV_{\mathrm{Class}}(t)}{UY_{\mathrm{Class}}(t)} \tag{3}$$

$$EVP_{\mathrm{Class}}(t) = EVA(t)PF_{\mathrm{Class}}(t) \tag{4}$$

C. ELECTRICITY PRICE AND CHARGING/BS FACILITY MODULE

This submodule mainly includes two parts of electricity price and charging/BS facilities. On the one hand, considering that $EP_{\mathrm{C}}(t)$ is relatively stable, the retail electricity price $EP_{\mathrm{R}}(t)$ is determined by charging/BS profit margin C_{PM} and $EP_{\mathrm{C}}(t)$. $EP_{\mathrm{C}}(t)$ is determined by $PSE(t)$, CC_{Class}, and IOC_{Class}.

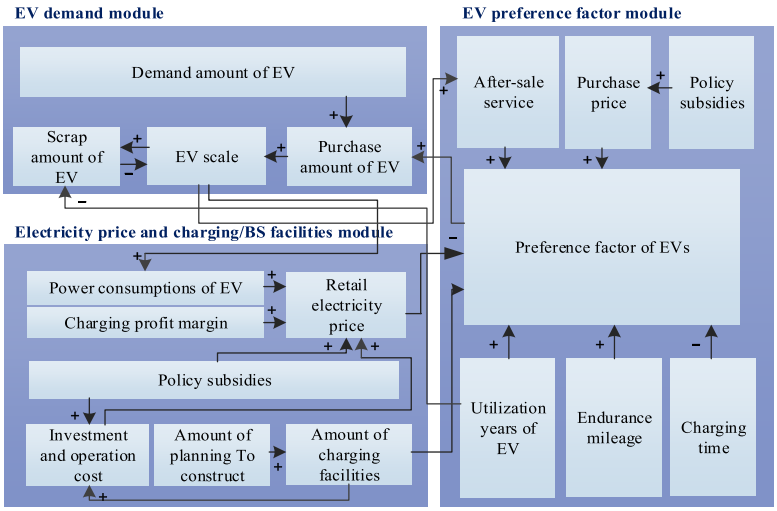

FIGURE 1. Causality relationship diagram for EV scale simulation.

Considering that HEV is powered by both electricity and gas, MI_{H} is larger than 1. BSEVs and PEVs are only powered by electricity. Thus, MI_{BS} and MI_{P} are equal to 1. Different IOC_{Class} indices of quick charging piles, slow charging piles, and BSSs are provided in [48]. The government will provide 30% subsidies of the facility investment for the operation business [65], which is expressed by $PSI(t)$. The relationships of these variables are shown in (5) and (6). On the other hand, $CFA_{\mathrm{Class}}(t)$ is determined by the number of charging/BS facilities in the former year $CFA_{\mathrm{Class}}(t-1)$, PA_{Class}, and $EVPR_{\mathrm{Class}}$, which is shown in (7). If the actual vehicle pile or vehicle station ratio $AVPR_{\mathrm{Class}}$, which is established by $EV_{\mathrm{Class}}(t)$ and $CFA_{\mathrm{Class}}(t)$, is larger than $EVPR_{\mathrm{Class}}$, $CFA_{\mathrm{Class}}(t)$ will be solely determined byPA_{Class}. Otherwise, an additional part of facilitiesEXA_{Class} will be added.

$$EP_{\mathrm{R}}(t) = C_{\mathrm{PM}} EP_{\mathrm{C}}(t) \tag{5}$$

$$EP_{\mathrm{C}}(t) = PSE(t) MI_{\mathrm{Class}} CC_{\mathrm{Class}} + IOC_{\mathrm{Class}}(1 - PSI(t)) \tag{6}$$

$$CFA_{\mathrm{Class}}(t) = \begin{cases} PA_{\mathrm{Class}} + CFA_{\mathrm{Class}}(t-1) \\ \qquad AVPR_{\mathrm{Class}} > EVPR_{\mathrm{Class}} \\ PA_{\mathrm{Class}} + EXA_{\mathrm{Class}} + CFA_{\mathrm{Class}}(t-1) \\ \qquad AVPR_{\mathrm{Class}} \le EVPR_{\mathrm{Class}} \end{cases} \tag{7}$$

D. EV PREFERENCE FACTOR MODULE

As the factors are demonstrated in section A, $PF_{\mathrm{Class}}(t)$ is determined by 7 main factors, which are endurance mileage $EM_{\mathrm{Class}}(t)$, charging/BS accessibility $CA_{\mathrm{Class}}(t)$, charging/BS time $CT_{\mathrm{Class}}(t)$, utilization life $UL_{\mathrm{Class}}(t)$, after-sale service $RBE_{\mathrm{Class}}(t)$, purchase price $PP_{\mathrm{Class}}(t)$, and driving price $DP_{\mathrm{Class}}(t)$. These factors are indexed from 1 to 7 in order. $EM_{\mathrm{Class}}(t)$, $CT_{\mathrm{Class}}(t)$, and $UL_{\mathrm{Class}}(t)$ are separately affected by the related coefficient of technology development $TD_{\mathrm{EM}}(t)$, $TD_{\mathrm{CT}}(t)$, and $TD_{\mathrm{UL}}(t)$. The function of technology maturity shows regularity [49]. Thus, the improvement percent of $EM_{\mathrm{Class}}(t)$, $CT_{\mathrm{Class}}(t)$, and $UL_{\mathrm{Class}}(t)$ are separately driven by $TD_{\mathrm{EM}}(t)$, $TD_{\mathrm{CT}}(t)$, and $TD_{\mathrm{UL}}(t)$. $TD_{\mathrm{EM}}(t)$, $TD_{\mathrm{CT}}(t)$, and $TD_{\mathrm{UL}}(t)$ are all set to 7% in each year [49]. In addition, the $UL_{\mathrm{Class}}(t)$ of PEVs, HEVs, and BSEVs are different, which are mainly determined by battery life. Thus, the $UL_{\mathrm{Class}}(t_0)$ of PEVs, HEVs, and BSEVs are respectively set to 7 years, 8 years, and 10 years. t_0 represents the initial year. Besides, the battery of BSEV is rent and the battery can keep a relative higher capacity, which is set as 80% [24]. $RBE_{\mathrm{Class}}(t)$ increases with $EV_{\mathrm{Class}}(t)$. $PP_{\mathrm{Class}}(t)$ is mainly determined by policy subsidies $PPS_{\mathrm{Class}}(t)$ in the short time and influenced by $TD_{\mathrm{PP}}(t)$. Finally, $DP_{\mathrm{Class}}(t)$ is composed of $EP_{\mathrm{R}}(t)$ and retail gasoline price $GP_{\mathrm{R}}(t)$. All descriptions related to the factors are shown as in (8)-(16). $\beta_{\mathrm{i}}(t)$ is the conversion coefficient corresponding to factor i. The smaller the number i, the larger weight the factor. θ_{EP} and θ_{GP} are the conversion weights of $EP_{\mathrm{R}}(t)$ and $GP_{\mathrm{R}}(t)$.

$$DP_{\mathrm{H}}(t) = \theta_{\mathrm{EP}} EP_{\mathrm{R}}(t) + \theta_{\mathrm{GP}} GP_{\mathrm{R}}(t) \tag{8}$$

$$PF_{\mathrm{Class}}(t) = \sum_{i=1}^{7} f^{i}_{\mathrm{class}}(t) \tag{9}$$

$$f^{1}_{\mathrm{Class}}(t) = EM_{\mathrm{Class}}(t) \beta_1(t) TD_{\mathrm{EM}}(t) \tag{10}$$

$$f^{2}_{\mathrm{Class}}(t) = CA_{\mathrm{Class}}(t) \beta_2(t) \tag{11}$$

$$f^{3}_{\mathrm{Class}}(t) = CT_{\mathrm{Class}}(t) \beta_3(t) TD_{\mathrm{CT}}(t) \tag{12}$$

$$f^{4}_{\mathrm{Class}}(t) = UL_{\mathrm{Class}}(t) \beta_4(t) TD_{\mathrm{UL}}(t) \tag{13}$$

$$f^{5}_{\mathrm{Class}}(t) = RBE_{\mathrm{Class}}(t) \beta_5(t) \tag{14}$$

$$f^{6}_{\mathrm{Class}}(t) = (PP_{\mathrm{Class}}(t) - PPS_{\mathrm{Class}}(t)) \beta_6(t) TD_{\mathrm{PP}}(t) \tag{15}$$

$$f^{7}_{\mathrm{Class}}(t) = DP_{\mathrm{Class}}(t) \beta_7(t) \tag{16}$$

Combining three parts of modules with three kinds of EVs, the stock-flow diagram for EV scale simulation is built via VENSIM and shown in Figure 2.

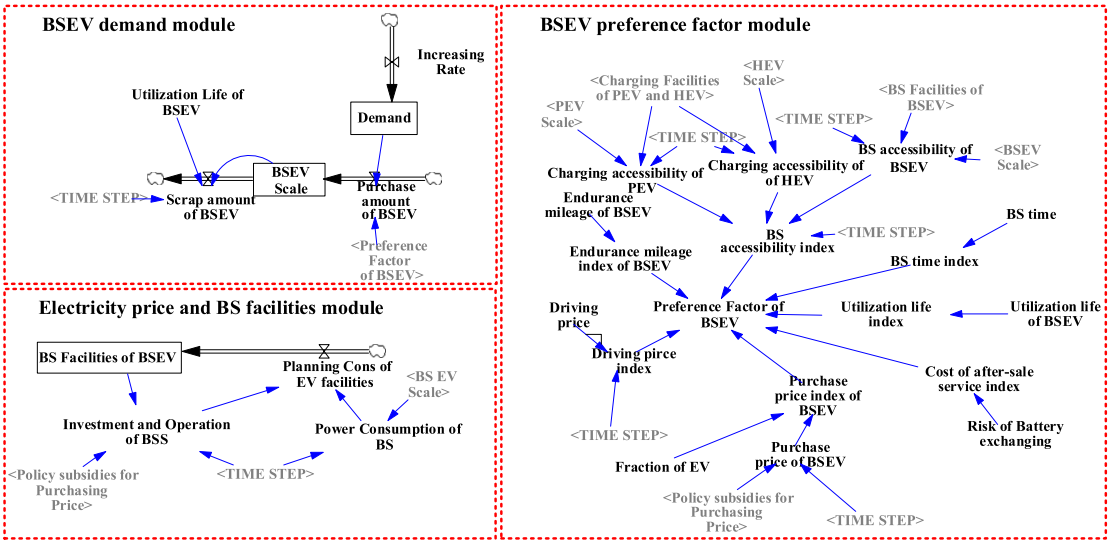

FIGURE 2. System dynamics model for BSEV scale simulation.

III. SPATIAL-TEMPORAL DISTRIBUTION OF BSEV SERVICE DEMAND BY SR METHOD

Service capacities of most energy supply stations are determined by their accessibility, when the market is stable and fair. For BSS, its accessibility mainly depends on the distance between BSSs and BSEVs. When the BS price is stable in a certain area, the closer the BSEV is to the BSS, the higher the BSS service accessibility will be. Thus, the service radius of BSS R_{BSS} is defined as an adaptive index for ruling the service capacity of BSS. The BS possibility P_{BS} for a BSEV driver to swap battery is determined by the number of BSS and the distance to BSS. When there is only one BSS in a certain location, distance will be the unique constraint. The maximum service radius $R_{\max}$ is used to evaluate the service accessibility of a BSS, which means a BSEV driver will not choose this BSS once the distance between BSEV and BSS is beyond $R_{\max}$. When the service radius is smaller than $R_{\max}$, P_{BS} will be influenced by the service radius. Figure 3 shows a relationship between number of BSSs and their service radius according to the left ordinate [29]. In different service radiuses, the number of BSSs can approximately reflect the P_{BS} of BSSs. According to Figure 3, $R_{\max}$ is set to 5km, and the ratios of P_{BS} against different service radiuses are shown in Figure 3 by exponential fitting.

Besides, the service capacity of BSSs is not only related to the actual distance between BSS and BSEVs. If the service ranges of different BSSs are overlapped, they will share these common BSEV resources together. For a BSEV driver, if there are two or more accessible BSSs at one location, all these BSSs can probably be chosen to serve according to the corresponding possibilities in terms of P_{BS} of each BSS. Meanwhile, these accessible BSSs will contribute to improving the service accessibility of corresponding locations.

The service accessibility factor $F^{j}_{\mathrm{SC},i}$ can be determined in (17). In (17), D_{BSS} represents the distance from a certain

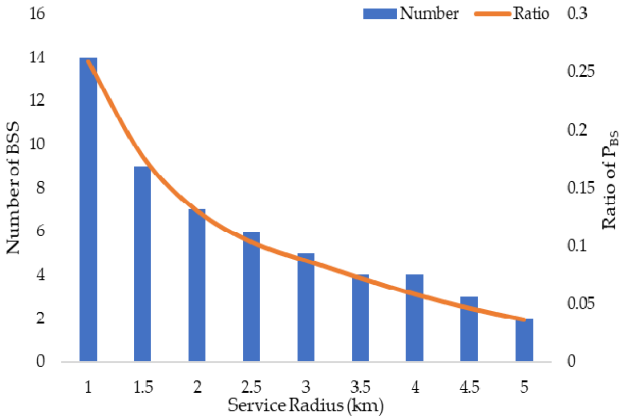

FIGURE 3. Relationship among SR, P_{BS}, and R_{BSS}.

location to one BSS. L is the total optimal planning locations of BSS. k is correlation coefficient, which is set to 0.095. i and j separately represent the ith accessible BSS and jth selectable planning location.

In order to calculate the service accessibility of each location, all BSSs in the entire area need to be considered together. The contributions of all accessible BSSs to the jth location are shown in (18).

$$F^{j}_{\mathrm{SC},i} = \begin{cases} ke^{-D_{\mathrm{BSS}}} & D_{\mathrm{BSS}} \le R_{\mathrm{MAX}} \\ 0 & D_{\mathrm{BSS}} > R_{\mathrm{MAX}} \end{cases} i \in N, \quad j \in L \tag{17}$$

$$F^{j}_{\mathrm{SC}} = \sum_{i=1}^{I_{\mathrm{BSS}}} F^{j}_{\mathrm{SC},i}, j \in L \tag{18}$$

As the demand for promoting the sustainable development and execution of the relative renewable policies, a high coverage area range of BSSs is the major premise. Thus, the service range is an important factor when determining locations of

BSSs [50]. To this end, the coverage range percent of BSSs $C_{\mathrm{R,BSS}}$ is set to balance the F^j_{SC} of BSS.

After the locations of BSSs are determined, $C_{\mathrm{R,BSS}}$ can be calculated. In (19), C^j_{R} is used to determine if there are accessible BSSs in location j. $C_{\mathrm{R,i}}$ and $P_{\mathrm{R,BSS}}$ can be calculated as in (20) and (21). $C_{\mathrm{R,i}}$ means the service degree of the ith BSS within the entire region. $\mathrm{C_{R,Total}}$ represents the total number of all selectable locations in the entire region.

$$C^j_{\mathrm{R}} = \begin{cases} 1 & F^j_{\mathrm{SC}} > 0 \\ 0 & F^j_{\mathrm{SC}} = 0 \end{cases}, \quad j \in L \tag{19}$$

$$C_{\mathrm{R},i} = \sum_{j=1}^{L} C^j_{\mathrm{R},i}, i \in N, \quad j \in L \tag{20}$$

$$P_{\mathrm{R,BSS}} = \frac{\sum_{j=1}^{L} C^j_{\mathrm{R}}}{C_{\mathrm{R,Total}}} \times 100\% \tag{21}$$

When a BSEV is looking for BS service, a closer BSS is more likely to be considered. In a region, once the scale of vehicles is large enough, this proximity principle will be more prominent and obvious. Based on this consideration, the real-time service number of BSEV is directly related to their passing traffic flow. In order to estimate service number of BSEV, the temporal-spatial distribution of traffic flows needs to be determined first. The trip modes and energy supply process of BSEV are similar to the traditional vehicles because of the short BS time. Thus, the real traffic flow can generally reflect the BSEV traffic flow. The spatial distribution possibilities of BSEV for each location are calculated as in (22).

$$P^j_{\mathrm{L,BS}} = \frac{P^j_{\mathrm{L,Vel}}}{\sum_{i=1}^{L} P^i_{\mathrm{L,Vel}}}, \quad j \in L \tag{22}$$

As the demand for calculating the regional BSEV scale, the BSEV amount must be obtained at first. Considering the regional process of sustainable energies and competitions among different businesses, the distribution of BSEVs Tj BS in each location can be calculated via (23). S_{EV}, I_{Re}, I_{Co}, and N_{BS} respectively represent extension coefficient of EVs, regional index, competitive index, and the predicted BSEV scale.

$$T^j_{\mathrm{BS}} = \begin{cases} \dfrac{S_{\mathrm{EV}} I_{\mathrm{Re}} I_{\mathrm{Co}} N_{\mathrm{BS}} F^j_{\mathrm{SC}} P^j_{\mathrm{L,BS}}}{\sum_{i=1}^{L} F^i_{\mathrm{SC}}}, & C^j_{\mathrm{R}} = 1 \\ 0, & C^j_R = 0 \end{cases} \tag{23}$$

Combining the Fj SC of BSSs and regional BSEV amount, the service quantity of BSEVs in each BSS is shown in (24) and (25). $F_{\mathrm{Loc,i}}$ and $S_{\mathrm{BSS,i}}$ respectively represent the scope of service ratio and the BS demand of the ith BSS. C_{i} and N respectively represent service region of each BSS and the total number of BSSs. $C_{\mathrm{R,max}}$ is the maximum range of BSS. $C_{\mathrm{L,out}}$ is the overrange coefficient, which is used to describe the service range of BSSs beyond the region allowed for locating. $C_{\mathrm{L,out}}$ is set to 0.7.

$$F_{\mathrm{Loc},i} = \frac{C_{\mathrm{R,max}}}{C_{\mathrm{R},i} + C_{\mathrm{L,out}}(C_{\mathrm{R,max}} - C_{\mathrm{R},i})} \tag{24}$$

$$_{\mathrm{BSS},i} = F_{\mathrm{Loc},i} \sum_{j=1}^{C_{\mathrm{R},i}} \frac{T^j_{\mathrm{BS}} F^i_{\mathrm{SC}}}{\sum_{k=1}^{N} F^k_{\mathrm{SC}}}, \quad i \in N \tag{25}$$

Besides, the service capacity of BSS is limited by BS speed and BS quantity per unit time. Normally, it takes about several minutes for a BSEV to swap battery and each BSS owns about 2-4 BS lanes [24]. Thus, the maximum quantity for each BSS in an hour can be calculated via (26). T_{hour} and L_{BSS} are separately set to 4 minutes and 2 lanes. In addition, the service quantity for each BSS should not exceed Q_{max} in each hour.

$$Q_{\mathrm{max}} = \frac{T_{\mathrm{hour}} L_{\mathrm{BSS}}}{T_{\mathrm{BSS}}} \tag{26}$$

IV. DETERMINATION OF OPTIMAL LOCATION MODEL OF BSSS

A. INVESTMENT AND OPERATION COSTS OF BSSS

The investment cost is one of the most important parts for the optimal location of BSSs. Before the construction of BSSs, the initial planning investment and post operation investment are two major parts. On the one hand, the initial planning investment of BSSs mainly includes land cost and equipment cost. Assuming that the planning standards and service strategies of individual BSSs are the same, the equipment cost and operation cost are stable. Thus, the land cost will be the major factor to be optimized.

The land cost generally depends on the coverage size S_{Land} and land price per unit C_{Land}, which is shown in (27). Another part of investment cost is BSS equipment cost, mainly including construction cost and battery cost. Thus, the investment of land cost I_{In} can be calculated in (28) [42].

$$I_{\mathrm{Land}} = S_{\mathrm{Land}} C_{\mathrm{Land},\,j}, \quad j \in L \tag{27}$$

$$I_{\mathrm{In}} = \sum_{i=1}^{N} I_{\mathrm{Land},i} + N I_{\mathrm{Eq}} \tag{28}$$

The cost for purchasing additional batteries and the degradation cost of batteries in BSSs are also considered. It is assumed that each BSS always has available fully charged batteries when a BSEV comes in. The estimated minimum battery stock is set to 0.1C. C means the battery capacity. It is shown that the lifetime of a battery mainly depends on the number of charging times, the depth of discharge, and the speed of charging [56]. CCSs generally have higher charging efficiency than that in BSSs, as the number of charging units in BSS is limited. Generally, the battery life is about 550 cycles in BSM [57]. Then, the battery cost for each BS H_{B} in terms of battery degradation is calculated as in (29). C_{B} means the battery purchasing price.

$$H_{\mathrm{B}} = \frac{C_{\mathrm{B}}}{550} \tag{29}$$

To satisfy the specific requirements of BSS construction, each BSS needs to equip with more than 28 batteries for swapping demand [42]. Thus, the total investment I_{Total} converted in each year can be calculated as in (30), where r_0 means discount rate and y_c means the year of depreciation. r_0 and y_c are separately set to 7% and 15 years.

$$I_{\text{Total}} = (I_{\text{In}} + N_{\text{B}} C_{\text{B}}) \frac{r_0(1+r_0)^{y_c}}{(1+r_0)^{y_c} - 1} \tag{30}$$

Besides, the costs for both consumers and suppliers in each BS are composed of two parts, which are battery and electricity. For consumers, according to an existing operation mode [58], they mainly afford battery rent cost and BS service cost. The rent cost is generally fixed and the BS service cost mainly depends on traveling mileage. The cost for suppliers is related to battery purchasing, electricity price, and operation cost. Thus, the weekly sales volume $\text{C}_{\text{Pro,per}}$ and operating cost $\text{C}_{\text{Op,per}}$ for a BSEV can be obtained as shown in equations (31). M_{Week}, D_{E}, and D_{Sea} respectively represent the weekly mileage, mileage per kilowatt hour, and seasonal coefficient. According to related researches [66], M_{Week}, D_{E}, and D_{Sea} are respectively set to 200km, 4.46km/kWh, and 1.12. C_{BS} and C_{Re} represent the BS cost per time and battery rent cost in each month. C_{Re} is set to 458 yuan per month. W_{Mon} means the average number of weeks in each month, which is set to 4.34.

$$C_{\text{Pro,per}} = \frac{M_{\text{Week}} C_{\text{BS}} D_{\text{Sea}}}{0.85 D_{\text{E}} C} + \frac{C_{\text{Re}}}{W_{\text{Mon}}} \tag{31}$$

Before calculating the total profits in a long term, the annual converted investments of land and equipment cost need to be considered as well. Thus, the annual converted profit P_{An} is shown as (33).

$$I_{\text{C}} = \frac{12}{y_c} \sum_{y=0}^{y_c} \frac{(C_{\text{Pro,per}} - H_{\text{B}}) W_{\text{Mon}} \sum_{i=1}^{N} S_{\text{BSS},i}^{y}}{(1+r_0)^{y_c}} \tag{32}$$

$$P_{\text{An}} = I_{\text{C}} - I_{\text{Total}} \tag{33}$$

B. ECONOMIC OPTIMAL LOCATION OF BSSS BY IDEA-MCS METHOD

After analyzing the service capacity as well as investment and operation cost of BSSs, the regional optimal location problem of BSSs aims to seek the locations of BSSs while satisfying the maximum annual profits and the maximum coverage range of BSSs, which is mainly limited by the coverage area of BSSs, the distribution of land price, and traffic flow. Thus, it is a multi-objective optimization problem.

In order to obtain the optimal locations of BSSs, the calculation accuracy is the major concern, which directly determines the service range and future profitability of BSSs. Because of the highly irregular distributions of land price and traffic flow, it is extremely difficult to derive exact results by analytical methods. To simplify the calculation process and promote the practicability of the model, the intelligent algorithm is widely used to search for optimal results [59]. However, once the problem presents a complex solution domain, it could be easily trapped into local-optimization. Improvements in searching scope and accuracy are presented in some studies [60]–[62]. In addition, another set of choices is ergodic methods, in which the most representative method is Monte Carlo method. It could provide solutions with higher quality, while sacrificing more computing time. Thus, simply using intelligent algorithms or ergodic method is unreasonable, and an IDEA-MCS method is established combing intelligent method with Monte Carlo method.

1) INITIALIZATION

The individuals of the entire population are two-dimensional coordinate values of BSS positions. The constraints of service range and non-overlapped locations of BSSs in the same population are considered. Then, $C_{\text{R,BSS}}$ is limited to no less than 0.5, and each position of all BSSs must be different. After all initial populations are randomly generated based on the constraints, the individuals of each population will be arrayed according to the coordinates in descending order, which will facilitate the process of crossover and mutation.

2) MUTATION

The traditional mutation method concentrates more on the changes among each number in finite dimensions. However, the individuals in populations represent the positions of BSSs. Using original mutation operators may easily lead to boundary convergence. A dynamic attractive mutation method considering the location relationships among individuals is established to generate new mutation individuals.

In order to describe the process of mutation for two-dimensional individuals, three different members, $p_{\text{r1}}(t)$, $p_{\text{r2}}(t)$, and $p_{\text{r3}}(t)$, are first chosen randomly from current populations. Next, the dynamic factor $g(t)$ and attractive mutation operator $v_{i,j}(t)$ are calculated in (34)-(35). $g(t)$ is generated randomly from t to GEN. t and GEN respectively represent number of current iterations and total number of iterations. $v_{i,j}(t)$ is created after the process that $p_{\text{r2}}(t)$ and $p_{\text{r3}}(t)$ attract $p_{\text{r1}}(t)$ in two-dimension. Typical value of F is in the range from 0.4 to 1.0.

$$g(t) = \frac{rand(t, GEN)}{GEN} \tag{34}$$

$$v_{i,j}(t) = (1 - g(t)) p_{r1,j}(t) + 0.5 g(t) (p_{r2,j}(t) + p_{r3,j}(t)) \tag{35}$$

3) CROSSOVER

To increase the diversity of the population, crossover operator is carried out, in which the donor vector exchanges its components with those of the current member $p_{\text{i}}(t)$. Two types of crossover could be used, including exponential crossover and binomial crossover. Although exponential crossover was presented in the original work of Storn and Price [63], the binomial variant is used more frequently in recent applications [64]. In this paper, binomial crossover scheme is used which can be expressed as in (36), where $u_{i,j}(t)$ represents a

child that will compete with the parent $p_{i,j}(t)$.

$$u_{i,j}(t)=\begin{cases} v_{i,j}(t), & if\ rand(0,1)<CR,\quad or\ rand(0,N)==i \\ p_{i,j}(t), & else \end{cases} \tag{36}$$

4) BOUNDARY TREATMENT

When the current child populations are generated, all individuals need to satisfy two basic constraints, which are location boundary constraint and individual non-repetitive constraint within each population. The location boundary constraint describes that once the individual is out of required positions, it will shrink to the nearest place as allowed. The individual non-repetitive constraint represents that once there are m (m is over 2) individuals in the same population, the other m-1 individuals of which will regenerate new positions within a small area of the origins, ultimately making individuals different. Due to coverage constraints, the small-range individual explosion will not occur.

5) GENERATING MCS OPERATORS

Due to the high complexity and nonlinearity of the problem, a direct global optimization by Monte Carlo method is unrealistic. Besides, simply increasing the numbers of iterations and population will not solve the problem of falling into local optimization. Therefore, compared with the traditional DEA method, the Monte Carlo searching (MCS) method is proposed to conduct a second optimization for some individuals in a small region. When the child $u_{i,j}(t)$ is obtained and one of the individuals changes within the permitted range, a better result might be found because of the randomness of initial population and crossover-mutation process. It can be achieved by MCS method. A principle sketch map is shown in Figure 4. The MCS method includes two main steps:

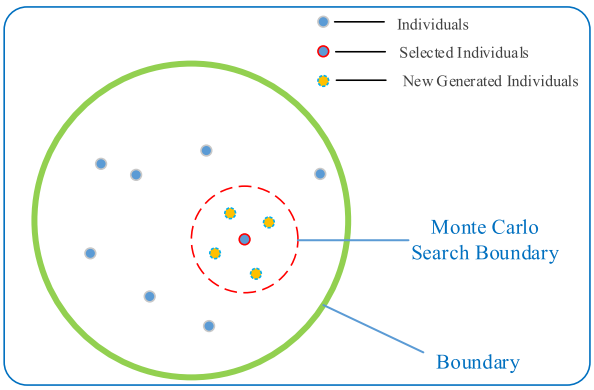

FIGURE 4. Monte Carlo searching method for one population.

Step 1: Select one individual from the child population randomly.

Step 2: Generate a new individual randomly within the concentric circle of MCS boundary. The center of the concentric circle is the selected individual, and the radius is dynamic determined by initial radius and *GEN*.

The details can be described via (37), where $u^s_{i,\mathrm{Sn}}(t)$ is a new generated point. As all positions are analyzed by Cartesian coordinate system, x and y are respectively horizontal and vertical coordinates. s is current search time.

$$\begin{aligned} u^s_{i,\mathrm{Sn}}(t) &= \{(x(t),y(t))|(x(t)-u_{i,j}(x(t)))^2 \\ &\quad +(y(t)-u_{i,j}(y(t)))^2 \le (6+n)^2, (x(t),y(t))\in L\}, \\ S_n(t) &= rand(1,N) \end{aligned} \tag{37}$$

6) SELECTION

To update the population, the fitness function of children and parents will be calculated. Considering the coverage degree of BSSs, it will be better when each BSS is not too close to others. Thus, a scope penalty factor F_{S} and a proximity penalty factor F_{P} are used to restrict locations of BSSs. Both F_S and Fi Pare penalty coefficients of I_{C}. F_s and Fi P are described as in (38) and (39).

$$F_{\mathrm{S}}=\begin{cases} 1 & if\ P_{\mathrm{R,BSS}}\ge 0.7 \\ \dfrac{P_{\mathrm{R,BSS}}}{0.7} & if\ P_{\mathrm{R,BSS}}<0.7 \end{cases} \tag{38}$$

$$F^i_{\mathrm{P}}=\begin{cases} 1 & \forall i\in N,\quad if\ D_{i,j}=0 \\ -1 & \forall i\in N,\quad if\ D_{i,j}>0 \end{cases} \tag{39}$$

Based on these results, the one with a larger value will survive in the next generation at time $t = t + 1$. The selection process can be expressed as in (40)-(41), where $f(\cdot)$ is the objective function to be maximized. If the child owns a better value of the fitness function, it will replace its parent in the next generation. Otherwise, the parent is retained in the next population. Hence the population is either improved in terms of a better fitness function or remains the same, but never deteriorates.

$$U_i(t)=\begin{cases} U_i(t), & if\ f(U_i(t))>f(U^s_i(t)) \\ U^s_i(t), & if\ f(U_i(t))\le f(U^s_i(t)) \end{cases} \tag{40}$$

$$P_i(t+1)=\begin{cases} U_i(t), & if\ f(U_i(t))>f(P_i(t)) \\ P_i(t), & if\ f(U_i(t))\le f(P_i(t)) \end{cases} \tag{41}$$

Finally, the flowchart for optimum planning of BSS is shown in Figure 5.

V. CASE STUDY AND DISCUSSION

A. CASE DESCRIPTION

The actual data of Beijing City is selected as an example to calculate the EV scale by SD model and optimal location of BSSs. It is assumed that BSEV, HEV, and PEV respectively response to three vehicle types of BYD Song [67]. The leased battery price of BSEV is 458 yuan per Month. Initial values of parameters adopted in the studies are shown in Table 3.

B. COMPARISON AMONG DIFFERENT EVOLUTIONAL SCENARIOS OF MULTI-TYPE EVS

After analyzing 16 recent years of car ownership in Beijing [13] and combining with a data fitting method for determining the growth rate [28], the car ownership in the

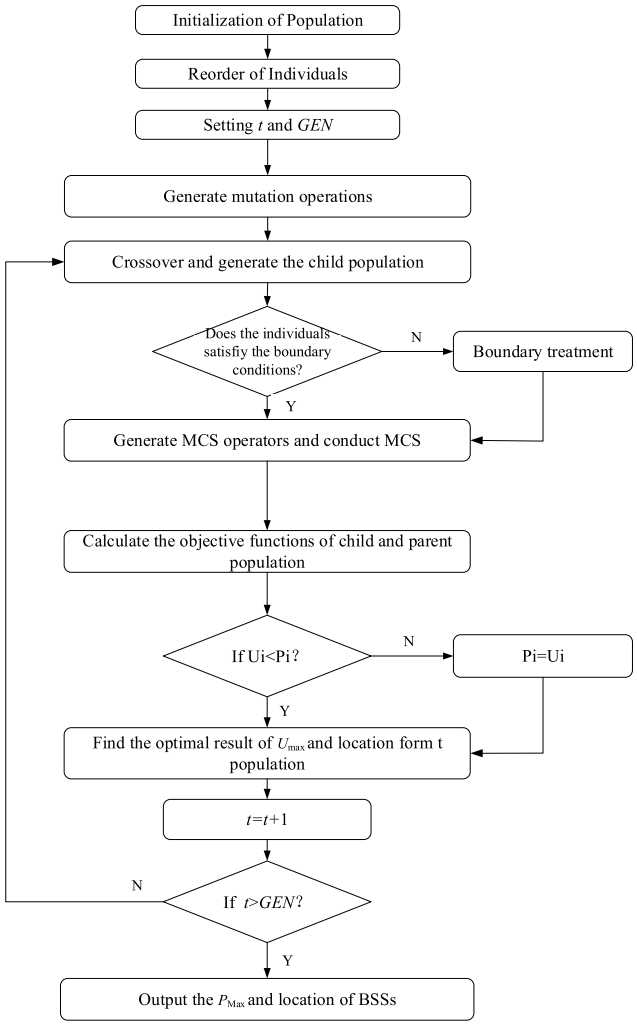

FIGURE 5. The flowchart of global economic optimum by IDEA-MCS method.

TABLE 3. Initial values of parameters.

Parameter name	Value	Parameter name	Value
C_{PM}	7%	S_{Land}	200m^2
H_B	227 $dollars	EP_R (t_0)	1.777 Yuan
PP_P	28.99×10^4 Yuan	GP_R(t_0)	7.80 Yuan
PP_{BS}	9.39×10^4 Yuan	$MI_{H\text{-}G}$	52 Lit
PP_H	20.25×10^4 Yuan	MI_P	61 kW·h
PPS	1.6×10^3 Yuan/kW·h	MI_{BS}	61 kW·h
CC	0.264 km/kW·h	$MI_{H\text{-}E}$	16 kW·h
I_{Eq}	3 million yuan		

future tens of years in Beijing can be approximated with a growth rate $R_I(t)$.

$$R_I(t) = 0.028 - 0.002t \tag{42}$$

Meanwhile, an optimistic scale, a normal scale, and a pessimistic scale of EVs are estimated in a region of a city [27]. Then it is further assumed that the peak of car ownership will come in 2030. According to different growth scenarios of EVs in the future, the growths of EVs under different scenarios are shown in Figure 6.

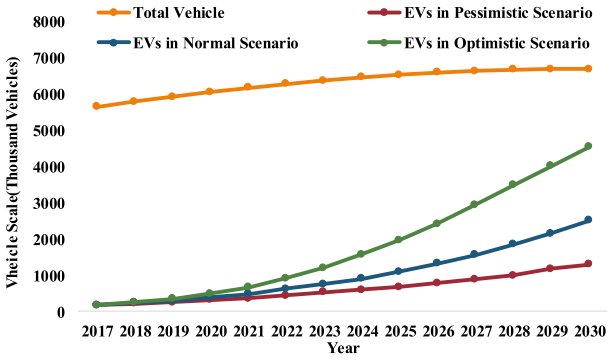

FIGURE 6. Evolutions of total vehicles and EVs.

After the evolution scale of total EVs estimated in different scenarios, the evolution scales of multi-type EVs are calculated by SD method, which are shown in Figures 7-9. The evolution results of BSEVs in different scenarios are compared in Figure 10. In these figures, although the initial amount of BSEVs is the lowest, the growth speed of BESV is obviously much faster than those of HEVs and PEVs. When the amount of BSEVs is larger than those of HEVs and PEVs, it will first happen at 2024, 2022, and 2021 respectively in pessimistic scenario, normal scenario, and optimistic scenario. It means that the faster the growth of total EVs, the earlier the BSEV will occupy the EV market. Meanwhile, PEV and HEV share similar growth speed in different scenarios.

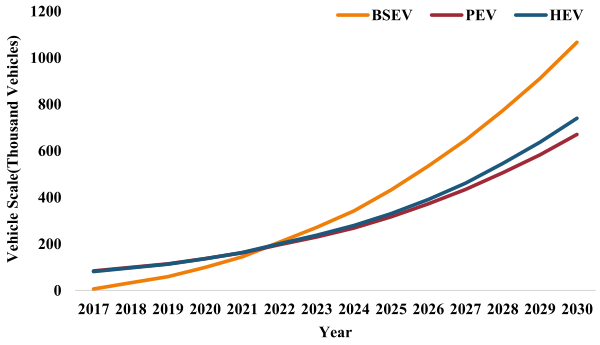

FIGURE 7. Evolution of multi-type EVs in normal scenario.

According to Figure 10, the amount of BSEV in optimistic scenario is about twice larger than that in normal scenario, and about four times larger than that in pessimistic scenario by 2030. Therefore, a rapider development of EVs will help BSEV take the lead in the EV market earlier as well.

Besides, the proportions of BSEVs in total EV scale in different scenarios are shown in Figure 11. According to Figure 11, even though the scales of BSEVs among different scenarios differ significantly, the proportions will gradually approach to around 42% by 2030.

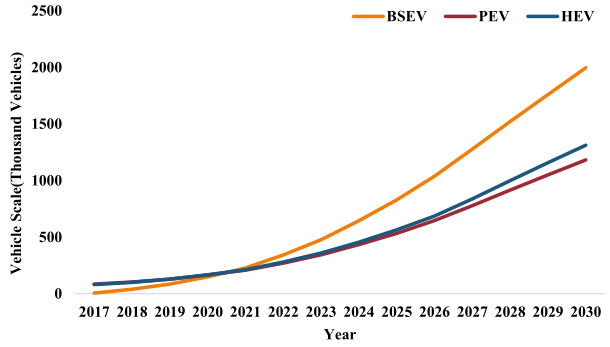

FIGURE 8. Evolution of multi-type EVs in optimistic scenario.

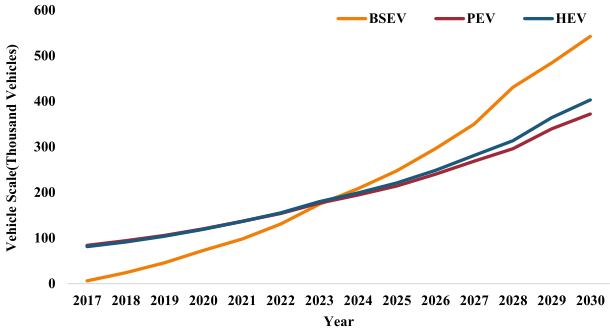

FIGURE 9. Evolution of multi-type EVs in pessimistic scenario.

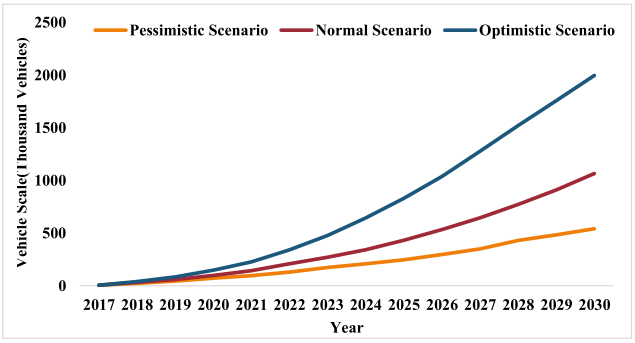

FIGURE 10. Evolution of BSEVs in different scenarios.

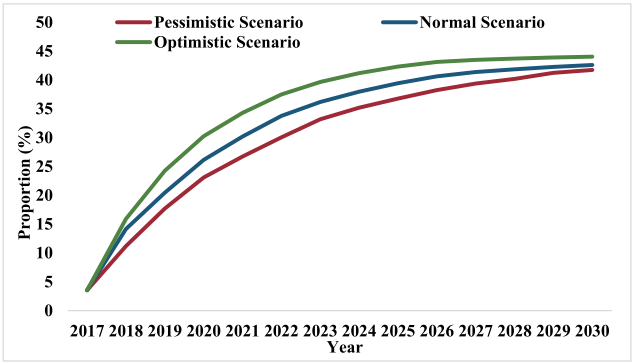

FIGURE 11. Proportion of BSEVs in total EV scale in different scenarios.

C. OPTIMAL LOCATION OF BSSS IN THREE DIFFERENT SCENARIOS

The data of land price in Beijing shows that the land price gradually decays from the center to surroundings in the year

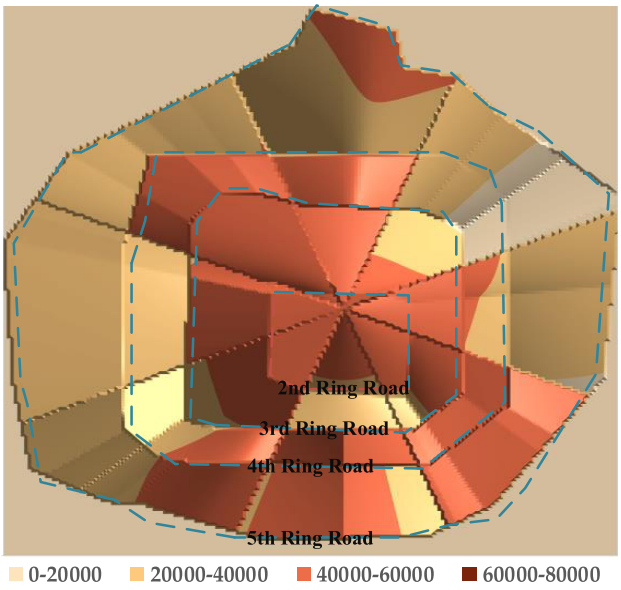

FIGURE 12. The distribution of land price in Beijing City.

of 2013 [53]. Meanwhile, based on 2017 investigation of land price in Beijing, the average commercial land price is about 30000 yuan per square meter within the 6th Ring Road [54]. Combining the analysis of decaying trade with the real land price, the estimated land price of analyzed area is shown in Figure 12. A typical traffic flow is counted by a large amount of data in Beijing [51], which shows the traffic flows in different periods of a week. This could roughly reflect the temporal distribution of BSEV quantity. Besides, the traffic conditions in an hour on Wednesday within the 5th Ring Road in Beijing City are recorded by traffic statistics. The numbers of vehicles within the 5th Ring Road take about 50% percent of total number of vehicles in Beijing [52]. Thus, I_{re} is set to 0.5. According to the analysis of energy development in Beijing city [68], the development of renewable energy is faster than those of most cities in China. Thus, S_{EV} is set to 1.5. Considering the competitiveness of BSEV market, I_{Co} is set to 0.5. When individual locations in a region share the same service accessibility of BSS, the scales of BSEVs in individual locations are distributed by spatial distribution of traffic flow. The temporal and spatial distributions of traffic flow are separately shown in Figure 13 and Figure 14. Then, the temporal and spatial proportional distribution regulations of BSEVs can be obtained according to the traffic flow of total vehicles.

As the targeted region is within the 5th Ring Road, the smallest unit for locating BSSs is set to a square with the size of 150m$\times$150m. About 28 thousand candidate locations can be selected as construction locations of BSSs. In order to validate the value of evolutional analysis on BSEV scale, the optimal results of P_{An}, $P_{R,BSS}$, and F_{Loc} among the SD method, linearized method, and simplified method in the pessimistic scenario are compared. It is considered that the gradient of the growth line of linearized predicted BSEV

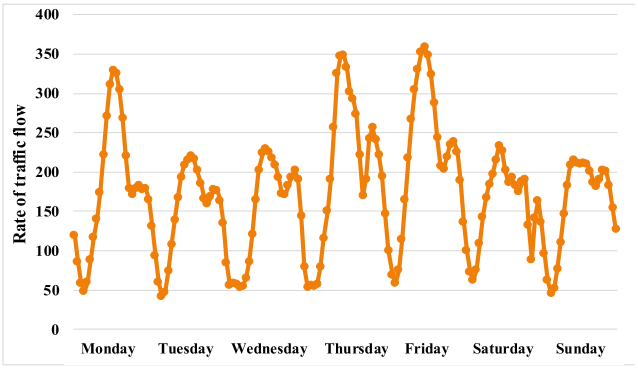

FIGURE 13. The temporal distribution of traffic flows.

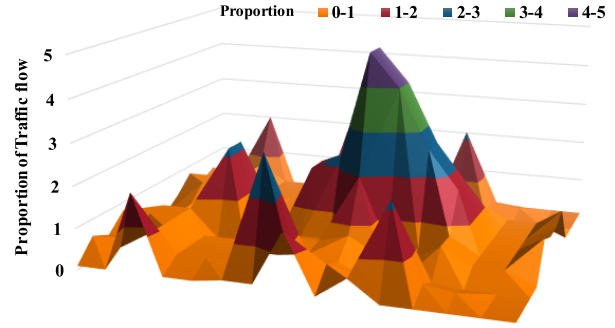

FIGURE 14. The spatial distribution of traffic flows.

scale evolution is determined by the gradient of the tangent point in the first year, which is obtained from the predicted BSEV curve by SD method. The predicted BSEV scale is determined by ignoring the HEV in the proposed model. The predicted BSEV scales by different methods are shown in Figure 15, and the comparisons on optimal results among SD method, linearized method, and simplified SD method are shown in Table 4.

TABLE 4. The comparison of optimal results among different method.

Scenario	SD Method	Linearized Method	Simplified Method
$P_{\mathrm{R,\,BSS}}$ (%)	60.10	61.36	61.85
F_{Loc} (%)	97.12	97.33	95.64
P_{An} (Yuan)	-3.532×10^6	-5.105×10^6	-1.123×10^6

As shown in Table 4, the results of $P_{\mathrm{R,BSS}}$ and F_{Loc} among different models are close. However, the results of P_{An} calculated by different methods are significantly different because of various sizes and growth speeds of predicted BSEV scales, which are shown in Figure 15. Therefore, an accurate model will provide a more reasonable future revenue assessment for investors and operators of BSSs.

Combined with the BSEV evolutional scales predicted in three different scenarios, three optimal planning schemes

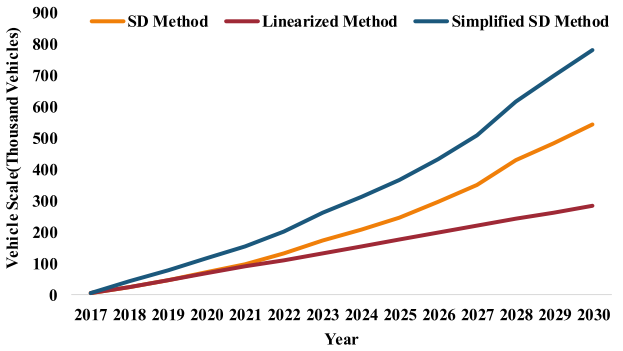

FIGURE 15. The predicted BSEV scales via different methods.

TABLE 5. Optimal results in different scenarios.

Scenario	Pessimistic scenario	Normal scenario	Optimistic scenario
$P_{\mathrm{R,\,BSS}}$ (%)	60.10	68.16	58.37
F_{Loc} (%)	97.12	96.89	87.40
I_{Total} (Yuan)	6.920×10^6	7.298×10^6	8.522×10^6
I_{C} (Yuan)	1.045×10^7	1.670×10^7	5.711×10^7
P_{An} (Yuan)	-3.532×10^6	9.779×10^6	4.925×10^7

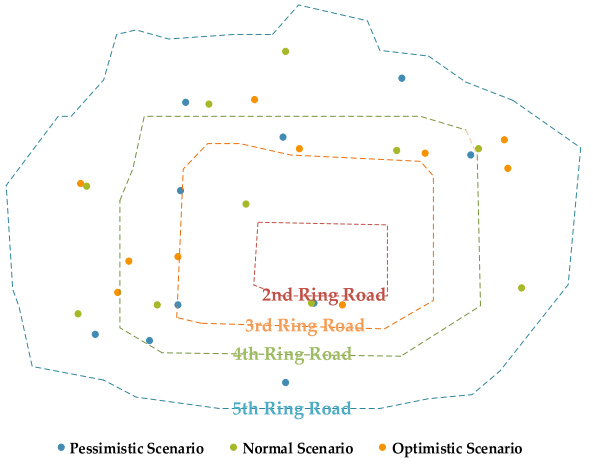

FIGURE 16. Optimal BSS location distribution in different scenarios.

of BSS locations are determined. The optimal annually converted profits and BSS location distribution are shown in Table 5, Figure 16, and Figure 17. In Table 5, the optimal results show that the optimal profits P_{An} in individual scenarios are quite different. The major reason is that the scales of BSEVs among different scenarios differ significantly, which directly impact the revenue of BSSs. Specifically, the optimal profit is negative in the pessimistic scenario, which means it may not be suitable to promote the BSM in a slow development area of EVs. On the other hand, the optimal profits in the optimistic scenario is preferable. In optimistic scenario, I_{Total} is the highest among three scenarios, while $P_{\mathrm{R,BSS}}$ and F_{Loc} are both the smallest. It can be explained as that once

TABLE 6. Cross-comparison of results under different scenarios.

Scenarios	Situational Replacement	Optimal Results (Yuan)	Converted Average Results (Yuan)
Pessimistic Scenario	Original Scenario	-3.532×10^6	2.902×10^7
	Normal Scenario	8.357×10^6	
	Optimistic Scenario	4.750×10^7	
Normal Scenario	Pessimistic Scenario	-3.622×10^6	3.389×10^6
	Original Scenario	9.779×10^6	
	Optimistic Scenario	4.834×10^7	
Optimistic Scenario	Pessimistic Scenario	-3.687×10^6	3.121×10^6
	Normal Scenario	9.035×10^6	
	Original Scenario	4.925×10^7	

the BSEV scale is large enough, the scale of traffic flow will make up the cost of land price so that the BSS could be located at an expensive land, which owns a higher rate of traffic flow.

In addition, the distributions of BSS locations among different scenarios are shown in Figure 16. According to Figure 16, the distributions of BSS locations among different scenarios are not similar with each other. It means that the optimal planning of BSS locations is greatly influenced by the scale of BSEVs. Besides, no BSSs are located within the 2nd Ring Road and more BSSs are distributed in the upper-left area in all scenarios, because the land is extremely costly or the rate of traffic flow is relative small within the 2nd Ring Road area, the bottom area, and right area in the entire region.

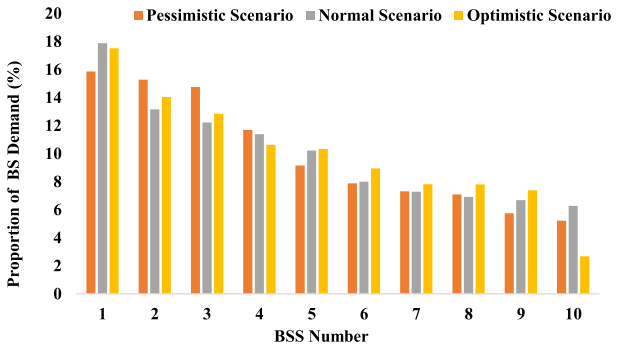

FIGURE 17. Proportion of BS demand in different scenarios.

Figure 17 shows the proportion of BS demands in each BSS in different scenarios and each BSS is numbered according to the proportion of BS demands. The proportions of BSS number 1 in normal scenario and optimal scenario are obviously higher than those in pessimistic scenario. Meanwhile, the proportion range in optimistic scenario is the largest. After calculating the standard deviations of the proportion of BSSs' BS demand, the standard deviation in optimistic scenario is also the top one compared with those in the other two scenarios, which means the BS orientation of BSEV in optimistic scenario is the most centralized. Although the proportion of BSS number 1 in normal scenario is the biggest, the standard deviation in normal scenario is the smallest. It is because the other 9 BSSs in normal scenario own low proportions of BS demand.

Based on these optimal distributions of BSSs, the optimal results of BSS locations in each scenario are brought into the other two scenarios for cross calculation and comparison, which are shown in Table 6. As the optimal profits show, the orders of magnitude of results in different scenarios are different. After cross-analyzing the results in three scenarios, the average optimal profits in different scenarios are calculated by leveraging the order of magnitude as in (44). The conversion coefficient C_1, C_2, and C_3 are calculated in (43), which separately are set to 1, 0.361, and 0.072 according to the proportionality relationship of P_{An} among pessimistic scenario, normal scenario, and optimistic scenario.

$$C_i = \frac{\left|P_{\mathrm{An},i}\right|}{P_1} \tag{43}$$

$$P_{\mathrm{An}}^{\mathrm{Sce}} = \sum_{i=1}^{S} C_i P_{\mathrm{An},i}^{\mathrm{Sce}} \tag{44}$$

As the average results show, the converted average result in normal scenario is the largest, while the converted average result in pessimistic scenario is the smallest. It means the optimal location of BSSs in normal scenario is more adaptable than those in the other scenarios, when the actual scenario is inconsistent with the predicted scenario. Therefore, when making the optimal location of BSSs, the analysis in normal scenario will be more instructive and practically useful.

D. ALGORITHM COMPARISON AND ANALYSIS

In order to verify the advantages of the proposed algorithm, three optimal methods, DEA, IDEA, and IDEA-MCS, are compared by calculating the global optimal planning of BSSs in the normal scenario. The results are shown in Figure 18, and the computational performance among these algorithms are shown in Table 7.

According to Figure 18, DEA method and IDEA method quickly converge to a local optimal result because of the large scale of this problem and the selection of initial population. However, a random individual is chosen by MCS method at

TABLE 7. Algorithm comparison of optimal results and calculation time.

Method	DEA	IDEA	IDEA-MCS
Optimal Result (10^6 Yuan)	9.3774	9.5135	9.7789
Calculation Time (hour)	5.028	7.139	27.528

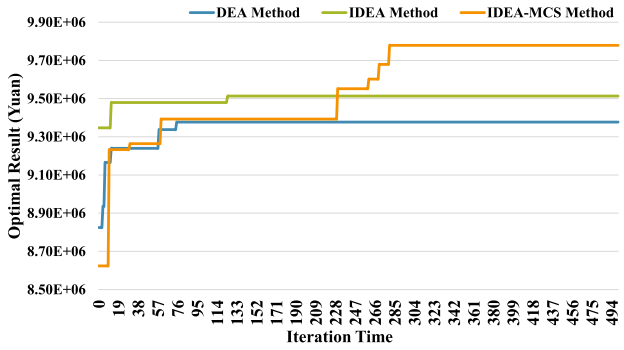

FIGURE 18. Algorithm comparison in normal scenario.

each iteration, which shows a stronger ability in searching a better result with a longer computational time.

Compared with DEA method and IDEA method for the optimal results and calculation time, the advantages and disadvantages of IDEA-MCS method are clear. On the one hand, the advantages of IDEA-MCS method are the fast convergence speed and strong capability in searching optimal results. On the other hand, the main disadvantage of IDEA-MCS method is the slow calculation speed. For the optimal BSS location planning problem, the superiority of results is much more important than the calculation speed. Therefore, the IDEA-MCS is valuable in calculating optimal locations of BSSs. The specific advantages and disadvantages of different methods are shown in Table 8.

TABLE 8. Advantages and disadvantages of different methods.

Method	Advantages	Disadvantages
DEA	Quite fast calculation speed	Quite weak searching capability, quite slow convergence speed
IDEA	Fast calculation speed, fast convergence speed	Weak searching capability
IDEA-MCS	Strong searching capability, quite fast convergence speed	Slow calculation speed

VI. DISCUSSION, CONCLUSION, AND PROSPECT

A. DISCUSSION

This paper discusses the prediction of multi-type EV scales in different scenarios by SD method and presents a SR method to estimate BSSs' BS demand. Furthermore, an IDEA-MCS method is proposed for optimizing the location of BSSs under the BSM via CCAUD to achieve maximum profit. The superiorities and limitations of the proposed methods are discussed as follows: 1) Compared with linearized method and simplified method, the prediction of multi-type EV scale in different scenarios by SD method could predict the scale of a specific type of EVs more reasonably and precisely. A limitation of the proposed method is that it needs the detailed consideration of all factors, which could potentially influence the evolution of EV scales. 2) The SR method is a BS demand-based method to estimate the spatial-temporal BS demand of BSSs. It is helpful to guide the operation and dispatching of BSSs. An accurate record and prediction of spatial-temporal traffic flows as well as a reliable model of BSEV drivers' service demand are the preconditions. 3) The IDEA-MCS method shows a strong searching capability and quite fast convergence speed on searching the optimal results of BSS profits and location planning. When the computing capability is weak, the calculation speed needs to be further improved.

B. CONCLUSION

Combined with the actual data in Beijing City, the predicted scales of multi-type EVs in three different scenarios are generated. The results show that the scale of BSEVs will grow faster than the scales PEVs and HEVs in all scenarios, and a rapider development of total EVs will help the BSEV take the lead in the EV market earlier. The proportions of predicted BSEVs in the total EVs in different scenarios will be closer in the future, which is about 42%. Furthermore, relying on the BSEV ownership data and the service demand of BSSs calculated by SR method, the optimal annual converted profit is obtained and BSS location distributions are determined among three evolution scenarios of BSEVs by the IDEA-MCS method, which combines with the data of spatial-temporal distribution of traffic flow and land price in Beijing City. The optimal distributions of BSSs in different scenarios are similar over a wide range, and the distribution of BSSs' BS demand in optimistic scenario is more inhomogeneous than those in the other scenarios. After cross-analyzing the results in different scenarios, the result in normal scenario shows a better adaptability compared with those in the other two scenarios. Finally, the IDEA-MCS method is compared to traditional DEA method and IDEA method, which shows a better capability in searching optimal solutions.

C. PROSPECT

On the basis of the study carried out in this paper, the future research work will be carried out from the following aspects: 1Ąjconsidering the complexity of influence factors for predicting the EV scale, it is necessary to further improve the rationality and accuracy of the relevant modeling. 2) Based on an accurate prediction of BSEV scale, a collaborative planning of BSS location, DG location, and power grid is quite significant for BSS investors and the power grid. 3) In order to obtain accurate BS or charging demand of EVs, building a more specific and reasonable BS or charging demand model

is of great benefits and assistances on electric energy management, while considering traffic data, EV drivers' demand, and some other related influences. 4) Because of the requirement of the faster calculation speed in operation process, an efficient and fast calculation algorithm method is urgently needed to deal with complex multi-objective optimization problems and ensure strong optimization capability.

REFERENCES

[1] J. Wang, A. J. Conejo, C. Wang, and J. Yan, "Smart grids, renewable energy integration, and climate change mitigation-future electric energy systems," *Appl. Energy*, vol. 96, pp. 1–3, Aug. 2012.
[2] Z. Hu, Y. Song, Z. Xu, Z. Luo, K. Zhan, and L. Jia, "Impacts and utilization of electric vehicles integration into power systems," *Proc. Chin. Soc. Elect. Eng.*, vol. 32, no. 4, pp. 1–10, Feb. 2012.
[3] K. G. Boroojeni, M. H. Amini, S. Bahrami, S. S. Iyengar, A. I. Sarwat, and O. Karabasoglu, "A novel multi-time-scale modeling for electric power demand forecasting: From short-term to medium-term horizon," *Electr. Power Syst. Res.*, vol. 142, pp. 58–73, Jan. 2017.
[4] M. H. Khooban, T. Niknam, and M. Sha-Sadeghi, "Speed control of electrical vehicles: A time-varying proportional–integral controller-based type-2 fuzzy logic," *IET Sci., Meas. Technol.*, vol. 10, no. 3, pp. 185–192, May 2016.
[5] G. A. Putrus, P. Suwanapingkarl, D. Johnston, E. C. Bentley, and M. Narayana, "Impact of electric vehicles on power distribution networks," in *Proc. IEEE Vehicle Power Propuls. Conf.*, Dearborn, MI, USA, Sep. 2009, pp. 827–831.
[6] F. Salah, J. P. Ilg, C. M. Flath, H. Basse, and C. van Dinther, "Impact of electric vehicles on distribution substations: A Swiss case study," *Appl. Energy*, vol. 137, pp. 88–96, Jan. 2015.
[7] X. Zhang, R. Rao, J. Xie, and Y. Liang, "The current dilemma and future path of China's electric vehicles," *Sustainability*, vol. 6, no. 3, pp. 1567–1593, Mar. 2014.
[8] O. Worley and D. Klabjan, "Optimization of battery charging and purchasing at electric vehicle battery swap stations," in *Proc. IEEE Vehicle Power Propuls. Conf.*, Chicago, IL, USA, Sep. 2011, pp. 1–4.
[9] Tencent Finance. (Dec. 15, 2014). *Charging Stations Achieving 15m Charging Have Been Established in Hangzhou*. [Online]. Available: http://finance.qq.com/a/20140224/000314.htm
[10] Haikou Website. (Dec. 15, 2014). *The First Battery Swapping Station Put into Operation in Haikou City*. [Online]. Available: http://haikou.hinews.cn/system/2013/03/19/015536425.shtml
[11] EV World. (Jan. 26, 2015). *Battery Swapping: The Undead or Still Viable Technology?* [Online]. Available: http://evworld.com/news.cfm?newsid=30677
[12] R. Rao, X. Zhang, J. Xie, and L. Ju, "Optimizing electric vehicle users' charging behavior in battery swapping mode," *Appl. Energy*, vol. 155, pp. 547–559, Oct. 2015.
[13] (Jan. 10, 2018). *Statistical Yearbook of Beijing*. [Online]. Available: http://tjj.beijing.gov.cn/nj/main/2018-tjnj/zk/indexch.htm
[14] Y. Cai, H. Wang, Q. Ye, and M. OuYang, "Business patterns of charging or swapping battery service for EV taxis in Shenzhen and Hangzhou in China," *J. Automot. Saf. Energy*, vol. 4, no. 1, pp. 54–60, Apr. 2012.
[15] M. R. Sarker, H. Pandžić, and M. A. Ortega-Vazquez, "Optimal operation and services scheduling for an electric vehicle battery swapping station," *IEEE Trans. Power Syst.*, vol. 30, no. 2, pp. 901–910, Mar. 2015.
[16] C. Gao, Q. Wu, F. Xue, and H. Liu, "Demand planning of electric vehicle battery pack under battery swapping mode," *Power Syst. Technol.*, vol. 37, no. 7, pp. 1783–1791, Jul. 2013.
[17] L. Zhang, S. Lou, Y. Chen, Y. Wu, and X. Huang, "Battery capacity optimization of electric vehicle battery swapping station based on leasing mode," *Power Syst. Technol.*, vol. 40, no. 6, pp. 1730–1735, Jun. 2016.
[18] S. Yang, J. Yao, T. Kang, and X. Zhu, "Dynamic operation model of the battery swapping station for EV (electric vehicle) in electricity market," *Energy*, vol. 65, pp. 544–549, Feb. 2014.
[19] Y. Liang and X. Zhang, "Battery swap pricing and charging strategy for electric taxis in China," *Energy*, vol. 147, pp. 561–577, Mar. 2018.
[20] C. Lianfu, W. Zhang, Y. Huang, and D. Zhang, "Research on the charging station service radius of electric taxis," in *Proc. IEEE Conf. Expo Transp. Electrific. Asia–Pacific*, Beijing, China, Aug./Sep. 2014, pp. 1–4.
[21] B. Qian, D. Shi, P. Xie, and L. Zhu, "Optimal planning of battery charging and exchange stations for electric vehicles," *Automat. Electr. Power Syst.*, vol. 38, no. 2, pp. 64–69, Feb. 2014.
[22] Y. Yang, Z. Hu, and Y. Song, "Research on optimal operation of battery swapping and charging station for electric buses," *Proc. Chin. Soc. Elect. Eng.*, vol. 32, no. 31, pp. 35–42, Nov. 2012.
[23] S. Zhang, Z. Hu, Y. Song, H. Liu, and M. Bazargan, "Research on unit commitment considering interaction between battery swapping station and power grid," *Proc. Chin. Soc. Elect. Eng.*, vol. 32, no. 10, pp. 49–55, Apr. 2012.
[24] T. Zhang, X. Chen, Z. Yu, X. Zhu, and D. Shi, "A Monte Carlo simulation approach to evaluate service capacities of EV charging and battery swapping stations," *IEEE Trans. Ind. Informat.*, vol. 14, no. 9, pp. 3914–3923, Sep. 2018.
[25] Y. Xiang, H. Zhou, W. Yang, J. Liu, Y. Niu, and J. Guo, "Scale evolution of electric vehicles: A system dynamics approach," *IEEE Access*, vol. 5, pp. 8859–8868, 2017.
[26] H. Zhou, "Analysis and simulation of electric vehicles scale evolution based on system dynamics," in *Proc. CSU-EPSA*, Aug. 2017, vol. 29, no. 8, pp. 1–7.
[27] W. Yang, Y. Xiang, J. Liu, and C. Gu, "Agent-based modeling for scale evolution of plug-in electric vehicles and charging demand," *IEEE Trans. Power Syst.*, vol. 33, no. 2, pp. 1915–1925, Mar. 2018.
[28] W. Yang, Y. Xiang, J. Liu, and Y. Li, "Multi-agent modeling for the scale evolution of plug-in electric vehicles," *Power System Technol.*, vol. 41, no. 7, pp. 2146–2154, Jul. 2017.
[29] J. Ma, N. Wang, and D. Kong, "Market forecasting study for new energy vehicle based on AHP and logit regression," *J. Tongji Univ. (Natural Sci.)*, vol. 33, no. 8, pp. 1079–1084, Aug. 2009.
[30] Y. Xue, J. Wu, D. Xie, K. Li, Y. Zhang, F. Wen, B. Cai, Q. Wu, and G. Yang, "Multi-agents modelling of EV purchase willingness based on questionnaires," *J. Mod. Power Syst. Clean Energy*, vol. 3, no. 2, pp. 149–159, Apr. 2015.
[31] I. Zelinka, L. Tomaszek, P. Vasant, T. T. Dao, and D. V. Hoang, "A novel approach on evolutionary dynamics analysis—A progress report," *J. Comput. Sci.*, vol. 25, pp. 437–445, Mar. 2018.
[32] V. J. Karplus, S. Paltsev, and J. M. Reilly, "Prospects for plug-in hybrid electric vehicles in the United States and Japan: A general equilibrium analysis," *Transp. Res. A, Policy Pract.*, vol. 44, no. 8, pp. 620–641, Oct. 2010.
[33] J. Yang and H. Sun, "Battery swap station location-routing problem with capacitated electric vehicles," *Comput. Oper. Res.*, vol. 55, pp. 217–232, Mar. 2015.
[34] J. Hof, M. Schneider, and D. Goeke, "Solving the battery swap station location-routing problem with capacitated electric vehicles using an AVNS algorithm for vehicle-routing problems with intermediate stops," *Transp. Res. B, Methodol.*, vol. 97, pp. 102–112, May 2017.
[35] C.-S. Liao, S.-H. Lu, and Z.-J. M. Shen, "The electric vehicle touring problem," *Transp. Res. B, Methodol.*, vol. 86, pp. 163–180, Apr. 2016.
[36] J. Yang, F. Guo, and M. Zhang, "Optimal planning of swapping/charging station network with customer satisfaction," *Transp. Res. E, Logistics Transp. Rev.*, vol. 103, pp. 174–197, Jul. 2017.
[37] F. He, D. Wu, Y. Yin, and Y. Guan, "Optimal deployment of public charging stations for plug-in hybrid electric vehicles," *Transp. Res. B, Methodol.*, vol. 47, pp. 87–101, Jan. 2013.
[38] S. S. Amiri, S. Jadid, and H. Saboori, "Multi-objective optimum charging management of electric vehicles through battery swapping stations," *Energy*, vol. 165, pp. 549–562, Dec. 2018.
[39] C. Liu, X. Wang, X. Wu, Y. Zou, H. Zhang, L. Yao, Y. Zhang, and Q. Cui, "Economic dispatch for microgrid with electric vehicles in plug-in charging and battery swapping modes," in *Proc. IEEE PES Asia–Pacific Power Energy Eng. Conf.*, Xi'an, China, Oct. 2016, pp. 1158–1163.
[40] U. Sultana, A. B. Khairuddin, B. Sultana, N. Rasheed, S. H. Qazi, and N. R. Malik, "Placement and sizing of multiple distributed generation and battery swapping stations using grasshopper optimizer algorithm," *Energy*, vol. 165, pp. 408–421, Dec. 2018.
[41] Q. D. Zhang, X. L. Huang, Z. Chen, L. X. Chen, and Y. P. Xu, "Research on control strategy for the uniform charging of electric vehicle battery swapping station," *Trans. China Electrotech. Soc.*, vol. 30, no. 12, pp. 447–453, Jun. 2015.
[42] Y. Tian, Q. Liao, Y. Xu, and Y. Chen, "Multi-scenario coordinated planning method of EV battery-swapping station and distributed generation based on coordinated charging strategy," *Electr. Power Automat. Equip.*, vol. 37, no. 9, pp. 62–69, Sep. 2017.

[43] X. Zhang, B. Zhang, and D. Liang, "Operation optimization of electric vehicles in battery swapping mode and direct charging mode in microgrid," *Automat. Electr. Power Syst.*, vol. 40, no. 9, pp. 56–63, May 2016.

[44] R. Khalilpour and A. Vassallo, "Planning and operation scheduling of PV-battery systems: A novel methodology," *Renew. Sustain. Energy Rev.*, vol. 53, pp. 194–208, Jan. 2016.

[45] J. J. Jamian, M. W. Mustafa, H. Mokhlis, and M. A. Baharudin, "Simulation study on optimal placement and sizing of battery switching station units using artificial bee colony algorithm," *Int. J. Elect. Power Energy Syst.*, vol. 55, pp. 592–601, Feb. 2014.

[46] Y Zhong, *System Dynamics*. Beijing, China: Science Press, 2009.

[47] Y. Tian and H. Zhuo, "Empirical study on influencing factors of purchasing decisions of electric vehicle consumers," *Market Weekly*, vol. 11, pp. 37–40, no. 11, pp. 37–40, Nov. 2014.

[48] Y. Zhuang, D. Yao, and Z. Zhao, "EV charging price mechanism," *East China Electr. Power*, vol. 42, no. 9, pp. 1937–1939, Sep. 2014.

[49] W. J. Carmack, L. A. Braase, R. A. Wigeland, and M. Todosow, "Technology readiness levels for advanced nuclear fuels and materials development," *Nucl. Eng. Des.*, vol. 313, pp. 177–184, Mar. 2017.

[50] (Oct. 9, 2015). *Electric Vehicle Charging Infrastructure Development Guide (2015–2020)*. [Online]. Available: http://www.ndrc.gov.cn/zcfb/zcfbtz/201511/t20151117_758762.html

[51] W. Chen, J. An, R. Li, L. Fu, G. Xie, M. Z. A. Bhuiyan, and K. Li, "A novel fuzzy deep-learning approach to traffic flow prediction with uncertain spatial–temporal data features," *Future Gener. Comput. Syst.*, vol. 89, pp. 78–88, Dec. 2018.

[52] (Jun. 9, 2017). *White Paper on Parking Industry Development in China*. [Online]. Available: http://www.gstachina.org/nd.jsp?id=508

[53] L. Shen, K. Ye, and C. Mao, *Proceedings of the 19th International Symposium on Advancement of Construction Management and Real Estate*. Berlin, Germany: Springer, 2015.

[54] (Jan. 1, 2018). *Analysis Report on Land Price Situation in Beijing in 2017*. [Online]. Available: http://www.ndrc.gov.cn/zcfb/zcfbtz/201511/t20151117_758762.html

[55] Q. Xu, Y. Kou, J. Ma, A. Yan, and M. Jian, "Research on typical design scheme of charging/battery swap infrastructure for electric vehicle," *Power Syst. Protection Control*, vol. 43, no. 13, pp. 118–124, Jul. 2015.

[56] S. B. Peterson, J. Apt, and J. F. Whitacre, "Lithium-ion battery cell degradation resulting from realistic vehicle and vehicle-to-grid utilization," *J. Power Sour.*, vol. 195, no. 8, pp. 2385–2392, Apr. 2010.

[57] S. S. Choi and H. S. Lim, "Factors that affect cycle-life and possible degradation mechanisms of a Li-ion cell based on $LiCoO_2$," *J. Power Sour.*, vol. 111, pp. 130–136, Sep. 2002.

[58] (Dec. 23, 2011). *Interim Measures for Demonstration and Promotion of Municipal Subsidies for Pure Electric Vehicles in Beijing*. [Online]. Available: http://fg.bjcz.gov.cn/bjlaw/loginAction do.

[59] A. Ahmad, S. Cuomo, W. Wu, and G. Jeon, "Intelligent algorithms and standards for interoperability in Internet of Things," *Future Gener. Comput. Syst.*, vol. 92, pp. 1187–1191, Mar. 2019.

[60] T. Ganesan, P. Vasant, and I. Elamvazuthi, *Advances in Metaheuristics: Applications in Engineering Systems*. Boca Raton, FL, USA, 2016.

[61] P. Vasant, I. Zelinka, and G. W. Weber, *Intelligent Computing & Optimization*. Berlin, Germany: Springer, 2019.

[62] P. Vasant, U. Kose, and J. Watada, "Metaheuristic techniques in enhancing the efficiency and performance of thermo-electric cooling devices," *Energies*, vol. 10, no. 11, p. 1703, Oct. 2017.

[63] R. Storn and K. Price, "Differential evolution-a simple and efficient heuristic for global optimization over continuous spaces," *J. Global Optim.*, vol. 11, no. 4, pp. 341–359, Dec. 1997.

[64] J. Vesterstrom and R. Thomsen, "A comparative study of differential evolution, particle swarm optimization, and evolutionary algorithms on numerical benchmark problems," in *Proc. Congr. Evol. Comput.*, Portland, OR, USA, Jun. 2004, pp. 1980–1987.

[65] (Dec. 18, 2017). *Rules for Subsidy Implementation of Electric Vehicle Charging Facilities in Shunyi District*. [Online]. Available: http://www.beijing.gov.cn/zfxxgk/syq11M002/dtxx52/201712/18/contentc61e5658220d4964b7b105f64d3f7bf1.shtml

[66] C. Gao, L. Zhang, F. Xue, and H. Liu, "Study on capacity and site planning of large-scale centralized charging stations," *Proc. Chin. Soc. Elect. Eng.*, vol. 32, no. 31, pp. 27–34, Nov. 2012.

[67] H. Dai, "The trend of BYD Song is coming," *Xinmin Weekly*, vol. 43, p. 80, Oct. 2015.

[68] (May 18, 2018). *Statistical Analysis of China's Electric Vehicle Charging Pile Industry in 2018 and Analysis of the Number Ranking of Charging Piles in Various Provinces and Municipalities*. [Online]. Available: http://chuneng.bjx.com.cn/news/20180518/898623.shtml

SHOUXIANG WANG (SM'12) received the B.S. and M.S. degrees in electrical engineering from the Shandong University of Technology, Jinan, China, in 1995 and 1998, respectively, and the Ph.D. degree in electrical engineering from Tianjin University, Tianjin, China, in 2001. He is currently a Professor with the School of Electrical and Information Engineering, and Deputy Director of Key Laboratory of Smart Grid of Ministry of Education, Tianjin University. His main research interests include distributed generation, microgrid, and smart distribution systems.

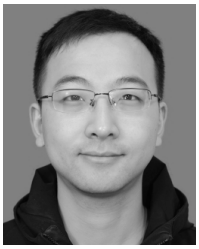

LU YU is currently pursuing the M.S. degree with the School of Electrical Automation and Information Engineering, Tianjin University, China. His research interests include renewable energy resources and distributed generation.

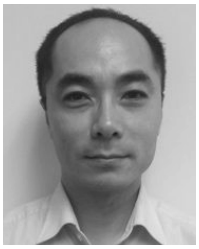

LEI WU (SM'13) received the B.S. degree in electrical engineering and the M.S. degree in systems engineering from Xi'an Jiaotong University, China, in 2001 and 2004, respectively, and the Ph.D. degree in electrical engineering from the Illinois Institute of Technology, USA, in 2008. He is currently an Associate Professor with the ECE Department, Stevens Institute of Technology. His research interests include power systems optimization and economics.

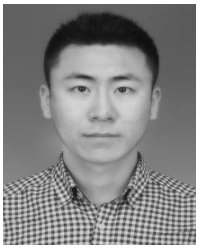

YICHAO DONG received the B.S. degree in electrical engineering from Tianjin University, Tianjin, China, in 2015. He is currently pursuing the Ph.D. degree with the School of Electrical and Information Engineering, Tianjin University. His research interests include distributed generation and distribution system planning.

HONGKUN WANG is currently pursuing the Ph.D. degree with the Key Laboratory of Smart Grid, Ministry of Education, Tianjin University. He is currently an Associate Professor with the College of Mechanical and Electrical Engineering, Shihezi University. His research interest includes smart distribution systems.